

Glow of own defects in ZnO polycrystals

N.L. Aluker

*FRC CCC SB RAS, Kemerovo, Russia
naluker@gmail.com*

Abstract. The photoluminescence of ZnO powders at room temperature upon excitation by microsecond pulses from the region of interband transitions and the region of exciton absorption has been studied. In the luminescence spectra, two regions characteristic of ZnO are observed: a short-wavelength region associated in the literature with exciton luminescence, and a long-wavelength region due to the presence of growth structural and impurity defects. The observed long-wavelength glow is divided into components with different glow durations, and several components that form this glow are identified. Experimental results and an analysis of the energy of formation and survival of the main structural defects make it possible to explain the luminescence of ZnO with allowance for the participation of only defects in the anionic sublattice and excitons in the process.

Keywords: photoluminescence, anion defects, polycrystalline zinc oxide.

1. Introduction

Zinc oxide (ZnO), a wide-gap semiconductor $E_g = 3.37$ eV, has attracted the attention of researchers for several decades due to a number of attractive applications, especially in optics and optoelectronics [1–3]. Although intriguing perspectives have led to extensive studies of ZnO structures, the nature of luminescence associated with major defects and impurities is still under discussion [1–5]. The study of defects is addressed again and again in the context of new applications, synthesis methods and studies that become available [4]. In various forms of zinc oxide, single crystals, films, powders, nanocrystals, and ceramics, two emission regions are recorded at different temperatures: a short-wavelength band near the fundamental absorption edge and a broad long-wavelength band determined by the presence of defects and impurities [1–9]. As reliably shown by low-temperature studies, short-wavelength luminescence is of an exciton nature. It is believed that due to the high binding energy of excitons (60 meV), this luminescence can be observed at room temperature and above [1, 6, 8, 10–12]. Long-wavelength luminescence is associated with various structural defects, such as oxygen vacancies, zinc vacancies, or interstitial oxygen and zinc atoms [13, 14], and certain impurities. A number of components of the long-wavelength range was established by introducing impurities (Cu, Li, etc.) that enhance the signal [11, 12].

Defects in the ZnO lattice can form during synthesis, high-temperature treatments, exposure to ionizing radiation (IR) and UV light in both the anionic and cationic sublattices. However, disstoichiometry with a pronounced n-type conductivity indicates stabilization in the lattice during the synthesis of neutral (stable) oxygen vacancies in the form of V_o^0 centers. Obtaining p-type ZnO is still problematic. Due to the non-stoichiometric composition of ZnO (deviation towards an excess of zinc or, more precisely, a lack of oxygen), varying the conditions of synthesis and treatments (thermo-, photo-, etc.) can lead to the formation of oxygen vacancies in different charge states (V_o^{++} , V_o^+ (F^+), V_o^0 (F)), which have different stability and provide a predictable change in properties [7, 15–18]. Oxygen vacancies and the change in their charge states during excitation, in our opinion, make the main contribution to the rather uniform, fundamentally the same for different degrees of purity, processing and study temperatures, dispersion, and luminescence of ZnO.

An analysis of the experimentally observed photoluminescence led us to the conclusion that for a consistent explanation of the luminescence of zinc oxide at room temperature, it is sufficient to have the excitation and ionization of only one stable structural defect, the F center. In this case, it is necessary to assume the possibility of radiative annihilation of an exciton in a regular lattice and on defects.

2. Details of the experiment

Photoluminescence was studied using a Fluorad 02 Panorama photoluminescent spectrometer. The light source of the analyzer is a high-pressure xenon lamp, which provides excitation in the mode of short (1 μ s) pulses. The operating wavelength range of the analyzer is 210–840 nm. The device contains two monochromators for excitation and registration of luminescence. The shape of the registered luminescence pulse depends on the luminescent properties of the sample and can either repeat the shape of the exciting pulse or be delayed with respect to the action of the exciting pulse. For luminescent measurements (quasi-stationary mode), the standard measurement mode is selected: pulse duration 1 μ s, delay 0.95 μ s (time during which the intensity of the lamp pulse increases), registration time interval 4.95 μ s (measuring gate). To measure luminescence longer than the drive pulse, the measuring gate can be as long as 1000 μ s, with a delay time relative to the sync pulse that triggers the lamp operation up to 6000 μ s.

Powdered samples of ZnO with a particle size of ~ 1 μ m were studied. The powders were pressed into a diaphragm 1 cm in diameter; the thickness of the densified layer was 3 mm. All samples of the same size and thickness were placed in the measurement compartment at an angle of 45 degrees, so the contribution of reflection to the observed signal was significant. Since the excitation was carried out in the region of fundamental or exciton absorption, the surface layer played an important role in signal formation. The luminescence spectra were measured for various excitations (band-band 3.49 eV) and the exciton absorption region 3.26 eV. For all luminescence bands observed in the spectrum, the excitation spectra and luminescence kinetics were studied.

Three types of powders were investigated: ZnO (1) chemically pure (chemically pure), ZnO (2) pure for analysis (analytical grade) and ZnO-Zn (3). The mass fraction of zinc oxide (ZnO) in both samples is at least 99.5% with a slightly higher content of Cl, Ca, Fe, Na and Cd impurities in the ZnO (2) sample. ZnO-Zn powder was obtained from a mixture of ZnO (2) powder with metallic Zn by recrystallization under the influence of a laser pulse in the ablation mode, i.e. high-temperature treatment of ZnO (2) in Zn vapor in air. ZnO and ZnO-Zn films were obtained by a similar deposition method.

To measure the absorption and reflection spectra, a SHIMADZU UV-3600 spectrophotometer was used. The optical density D is measured in the range 0–6, with an accuracy of 0.001. Wavelength range 185–3600 nm. Diffuse reflectance spectra were measured using an ISR-3100 integrating spherical nozzle. All measurements were performed at room temperature.

3. Results of experimental studies

3.1. Absorption

On Fig.1 shows the diffuse reflectance spectrum of ZnO (2) powder. Reflection (absorption) in the region of the Urbakh tail (3.26 eV) is much lower than in the region of intrinsic absorption.

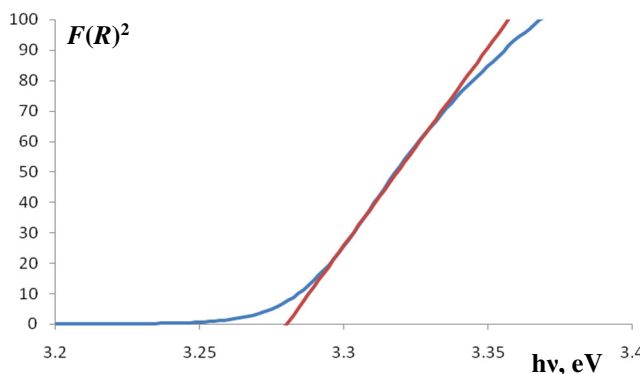


Fig.1. Diffuse reflection spectrum of ZnO-2 powder.

3.2. Luminescence during the action of an exciting pulse.

In the photoluminescence spectra of the initial powders, ZnO (1) and ZnO (2) of different purity, and the ZnO film, upon excitation in the zone-zone region (3.49 eV, 355 nm), under standard conditions for recording quasi-stationary luminescence, predominantly short-wavelength luminescence $E_{max} = 3.2 \pm 0.01$ eV, $\Delta = 0.15$ eV, with a smaller contribution of long-wavelength luminescence (Fig.2a). Unless otherwise specified, all subsequent measurements were performed under standard recording conditions.

In ZnO-Zn, this luminescence is quenched by about an order of magnitude. Long-wavelength luminescence becomes predominant, it is comparable in intensity with ZnO (2) and ~ 4 times higher than in ZnO (1) and the ZnO film. The duration of long-wavelength luminescence with an effective maximum $E_{max} = 2.53 \pm 0.02$ eV, $\Delta = 0.56$ eV exceeds the duration of the exciting pulse, which is well fixed by the difference in measurements with a short and long strobe (Fig.2b).

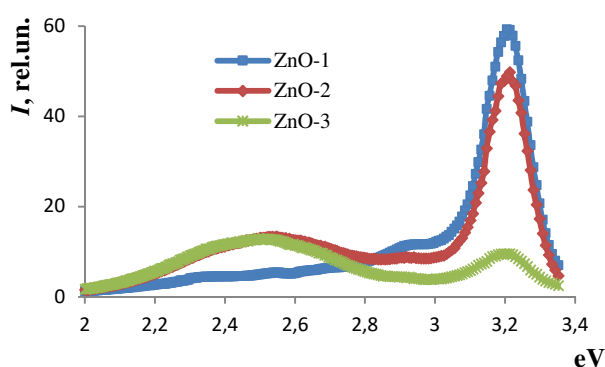


Fig.2a. Luminescence of ZnO powders upon excitation in the zone-zone region (3.49 eV) under standard registration conditions.

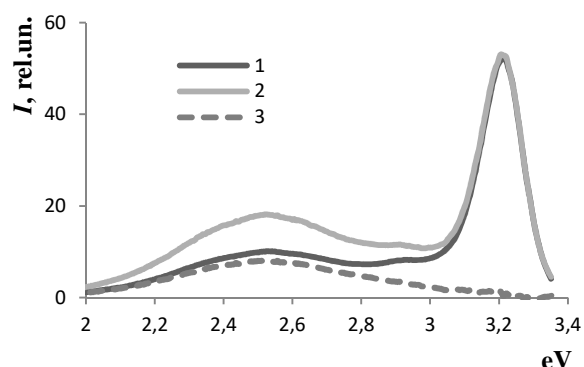


Fig.2b. Luminescence of ZnO (2) powder upon excitation into the zone-zone region (3.49 eV) under standard conditions (1), strobe duration 1000 μ s (2) and the difference between the spectra (3), showing the contribution of luminescence components with duration >4.95 μ s

3.3. Luminescence kinetics

Separation into components of non-elementary long-wavelength luminescence is well performed in terms of the delay times after the action of the exciting pulse and the duration of luminescence registration, i.e. in kinetic research.

A wide band with an effective maximum $E_{max} = 2.53 \pm 0.02$ eV, $\Delta = 0.56$ eV (Fig.2b) is quenched for 30 μ s (Fig.3a) after exposure to an excitation pulse by about 20 times, which makes it possible to distinguish luminescence bands of longer duration with effective maxima ~ 2.7 eV and ~ 2.34 eV (Fig.3a). When the delay is increased to 100 μ s, only long-term luminescence with an effective maximum of ~ 2.7 eV is recorded in the spectra (Fig.3b). A similar picture is also observed upon excitation at 3.26 eV (Urbach absorption edge).

Thus, a broad, non-elementary long-wavelength luminescence band of powders and films is formed by at least three luminescence bands with different contributions and durations. Fast luminescence is determined by the contribution of the band $E_{max} = 2.53 \pm 0.02$ eV, $\Delta = 0.56$ eV, in the afterglow bands with $E_{max} = 2.7 \pm 0.01$ eV, $\Delta = 0.4$ eV, $\tau \sim 500$ μ s are recorded, 2.34 eV, $\Delta = 0.6$ eV, $\tau \sim 100$ μ s and a weak long-wavelength glow in the region of 2.2–1.8 eV, $\tau \sim 100$ μ s. In the ZnO-Zn sample in the afterglow, the luminescence of 2.3 eV, $\Delta = 0.6$ eV and the long-wavelength luminescence of 2.2–1.8 eV are more clearly expressed.

In fast luminescence, in addition to the main bands of 3.2 eV and 2.53 eV, a weaker luminescence with a maximum is observed $E_{max} = 2.9 \pm 0.01$ eV, $\Delta = 0.15$ eV).

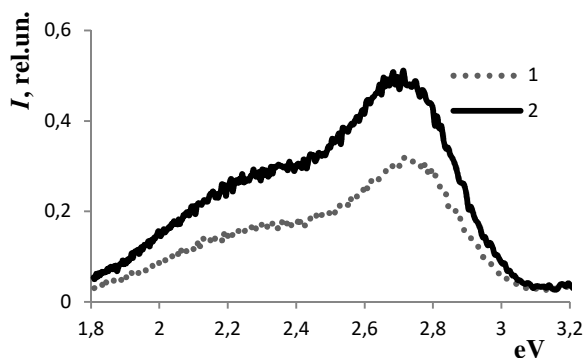


Fig.3a. Luminescence of ZnO (2) powder upon excitation into the zone-zone region (3.49 eV) with a gate delay of 30 μ s, a strobe duration of 100 μ s (1) and 1000 μ s (2).

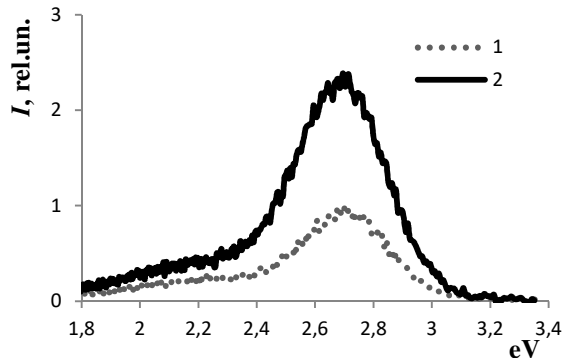


Fig.3b. Luminescence of ZnO (2) powder upon excitation into the zone-zone region (3.49 eV) with a gate delay of 100 μ s, a strobe duration of 100 μ s (1) and 1000 μ s (2).

Table 1 lists the characteristics of the bands observed in the luminescence of ZnO powders with an estimate of the duration of the luminescence and the intensity ratio of the bands during the action of the excitation pulse.

Table 1. characteristics of the bands

Maximum FL, eV (nm)	FWHM, Δ , eV	τ , μ s	I , relative units
3.2 ± 0.01 (387)	0.15	≤ 1	50
2.9 ± 0.01 (427)	0.15	≤ 1	6
2.7 ± 0.01 (460)	0.4	~ 500	~ 1
2.53 ± 0.02 (490)	0.5	≤ 1	12
2.34 ± 0.02 (530)	0.6	≤ 100	~ 1
(2.2–1.8) (560–690)		≥ 100	~ 0.2

3.4. Photoluminescence excitation spectra

The UV luminescence band is well excited in the spectral range of interband transitions with an effective maximum in the region of 4.32 eV. This broad excitation band has an oscillatory structure, which indicates a weak level localization and a strong influence of the environment. A slightly higher excitation efficiency is fixed in the region of the exciton absorption band. The excitation spectrum of long-wavelength luminescence with a maximum at 2.53 is similar to the excitation spectrum of short-wavelength luminescence at 3.2 eV (4a), with a pronounced short-wavelength excitation band at 4.5 eV and excitation in the exciton absorption region.

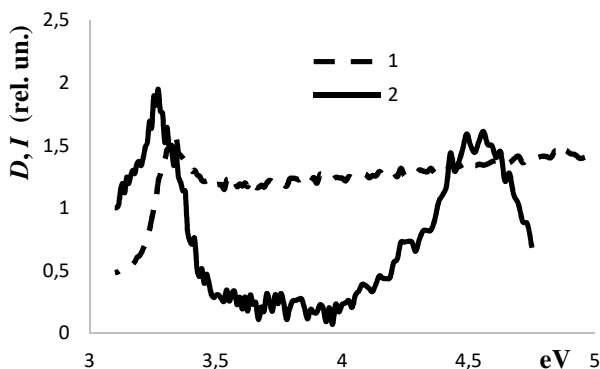


Fig.4a. Absorption spectra (dotted line) and 2.53 eV luminescence excitation spectrum (2) of a ZnO film under standard recording conditions.

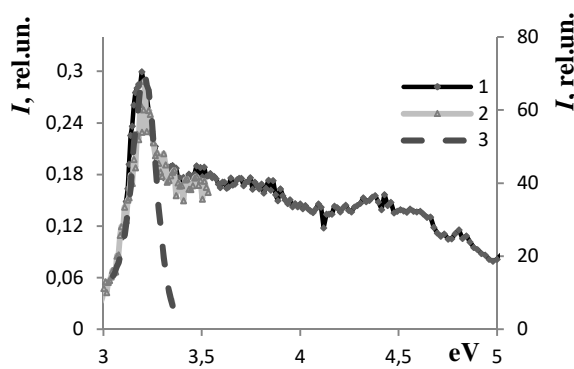


Fig.4b. Excitation of long-term luminescence with maxima 2.7 eV (1) and 2.34 eV (2) – left axis and fast luminescence upon excitation 3.49 eV (3) – right axis.

Long-term luminescence of 2.7 eV and 2.34 eV, along with weakly structured excitation in the band region, is effectively excited in the region of 3.2 eV, i.e. energy coinciding with the energy of UV luminescence (Fig.4b). It is quite probable that volume excitation occurs during the radiative annihilation of a localized (self-trapped) exciton in a sensitized process.

3.5. Dependence of luminescence on excitation density

In experiments at different excitation densities, a change in the luminescence spectra is traced, due to the ratio between the number of generated electronic excitations and growth defects. The yields of UV and long-wavelength luminescence depend differently on the intensity of the exciting light pulse. On Fig.5 shows the short-wavelength and long-wavelength luminescence spectra of the ZnO (1) powder corrected for the intensity of the excitation pulse at different excitation intensities (rel. units).

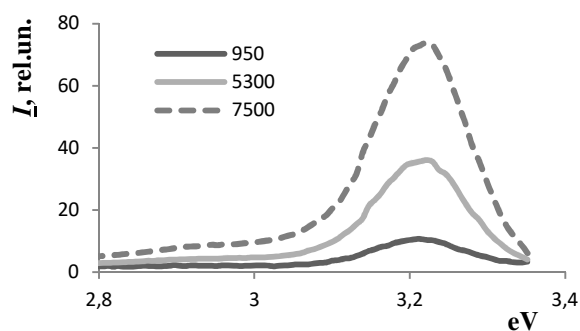


Fig.5a. Luminescence of ZnO (1) powder in the short-wavelength band upon excitation at 355 nm at different excitation intensities (rel. units), normalized to the excitation intensity under standard measurement conditions.

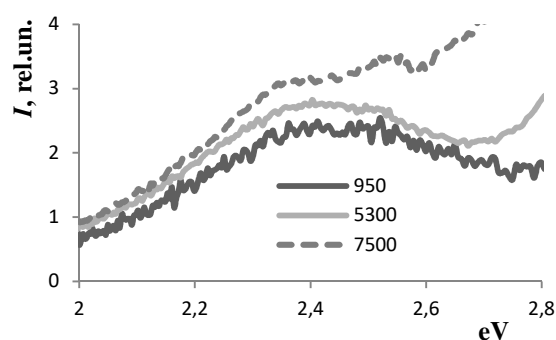


Fig.5b. Luminescence of ZnO (1) powder in the long-wavelength band upon excitation at 355 nm at different excitation intensities (rel. units), normalized to the excitation intensity under standard measurement conditions.

The long-wavelength luminescence yield weakly depends on the excitation intensity (i.e., the dependence of the luminescence intensity on the excitation intensity is linear), the dependence of the exciton luminescence yield is more complicated: the yield decreases at low intensities and linearly increases at high intensities (quadratic dependence). At very low excitation intensities, 2–3 orders of magnitude lower than the standard ones, only UV luminescence of the surface is observed, the yield reaches tens of percent and drops with an increase in the light pulse intensity to fractions of a percent. The glow is apparently due to the contribution of scattering to the measured signal.

A complex structured glow, possibly due to resonant Raman scattering of short and intense luminescence of a free exciton (3.28 eV) on gases adsorbed by the surface. If we accept this hypothesis, then the Raman bands can be associated with $\text{N}_2 - 598 \text{ cm}^{-1}$, 2330 cm^{-1} (387 nm, 414 nm), $\text{NO}_2 - 754 \text{ cm}^{-1}$, 1320 cm^{-1} (390 nm, 398 nm), $\text{OH} - 3355 \text{ cm}^{-1}$ (433 nm), $\text{H}_2 - 4130 \text{ cm}^{-1}$ (448 nm), i.e. manifest itself in the region from 390 to 440 nm, which is observed experimentally (Fig.6).

The conditions for observing luminescence and the use of powdered samples undoubtedly make it extremely sensitive to the state of the surface, the conditions of pretreatment of samples, and the sorption and desorption of atmospheric gases.

At medium intensities, a section of long-wavelength luminescence growth and a decrease in UV luminescence (competing processes) is observed. When long-wavelength luminescence reaches saturation, the increase in the UV luminescence yield continues. The saturation of long-wavelength luminescence in ZnO (2) (higher concentration of defects) occurs at a higher excitation intensity than in ZnO (1).

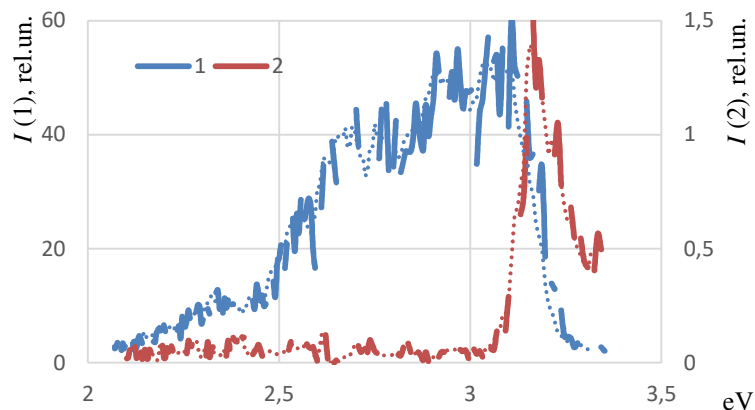


Fig.6. The luminescence of ZnO (1) powder normalized to the excitation intensity upon excitation of 3.49 eV at excitation intensities of 8 rel. units (1) and 27 rel. units (2), i.e. three orders of magnitude lower than those used under standard conditions (7000 rel. units).

The revealed regularities are of a fundamental nature and allow us to make a number of assumptions about the nature of the observed processes, which are given in the discussion.

4. Discussion

In dielectrics and semiconductors, intrinsic absorption has a complex structure, where the absorption of excitons is superimposed on the continuum of interband transitions.

To explain the luminescence characteristic of wide-gap oxides, the concepts of alternative mechanisms for the relaxation of electronic excitations associated with the self-trapping of free excitons or the recombination creation of STEs on a defect are used [15, 19]. The first photo mechanism is based on the creation of a free exciton and its relaxation into a self-trapped state. The second way is associated with the production of an exciton due to the recombination of electron-hole pairs. In oxides, the model of an exciton hole nucleus in the form of an O_2^- ion is considered. The absorption and luminescence of the STE are broadened and lie in the region of lower energies than the first exciton absorption peak. In some cases, conditions are created for the coexistence of free and self-trapped excitons. The higher the excitation density, the more likely the channel of the recombination pathway for exciton production becomes. In wide-gap semiconductors, which include ZnO, there are prerequisites for the coexistence of free and self-trapped excitons; in wide-gap oxides SiO_2 , Al_2O_3 , BeO , MgO , the participation of self-trapped excitons in energy conversion processes has been reliably proven. A small barrier probably exists for the self-trapping of a free exciton in ZnO. The presence of a barrier at helium temperatures prevents the exciton from being localized, and it radiatively annihilates in the hot, unrelaxed state. At room temperature, it is possible to observe both a free exciton and an exciton localized in a regular lattice, or at impurity and defect levels. The wide observed UV bands at cryogenic temperature, which are fixed depending on the excitation density and the dimensions of objects in the range from 370 to 390 nm, are most likely associated with the radiative annihilation of a relaxed exciton.

The F center is a quasi-stable formation in ZnO and has a local level in the band gap approximately 0.5 eV above the top of the valence band. The singlet state of the excited center ($F_s^* \sim 5$ eV) was in the conduction band, and the excited triplet state ($F_t^* \sim 3$ eV) was near the bottom of the conduction band. Due to the hole nature of the singly charged (VO^+ analogous to the F^+ center) and doubly charged (VO^{2+}) states and the presence of free electrons in the conduction band of ZnO, these centers can appear only during excitation when the F center is recharged. On the surface, due to the upward bending of the bands in the case of n-type

conductivity, the level of the F center is located near the top of the valence band, with the possibility of capturing a hole and producing an exciton. In the formation of ($F^+ e^-$) upon excitation, the processes of radiative exciton decay and intracenter excitation of the F center are competing.

It can be assumed that the 3.2 eV luminescence is associated with the radiative decay of an exciton at surface F centers or in a regular lattice. Luminescence 2.53 eV and 2.9 eV with electron recombination at the F^+ and V_O^{++} centers that appear during recharging of F-centers. Luminescence of 3.2 eV falling into the transparency region can lead to the excitation of bulk impurity and structural defects (2.34 eV, 2.2–1.8 eV), a. also, to the population of the triplet state of the F-center (2.7 eV). The longer wavelength luminescence bands that form the afterglow, in our opinion, can be due to vapors and impurity defects, as is considered in a number of works. Separated pairs $(O_i+V_O)_d^{oct}$ (~1eV) and $(O_i+V_O)_d^{tet}$ (0.75 eV) or $(Zn_i+V_{Zn})_d^{oct}$ can be stable defects in the ZnO lattice.

Luminescence of 3.2 eV, 2.53 eV, and 2.9 eV ($\leq 1 \mu s$) is caused by competing processes depending on the excitation density and the number of defects on the surface and in the bulk of the lattice. Edge radiation leads to the excitation of bulk defects and their luminescence (2.7 eV, 2.34 eV, 2.2–1.8 eV) $> 1 \mu s$.

The coexistence of free and self-trapped excitons and stable growth defects are sufficient conditions for describing the luminescence of ZnO. The UV band (~3.2 eV) is associated with the radiative decay of excitons, including at Fs centers, the bands at 2.9 and 2.53 eV with bulk F and F^+ centers or pairs. The wide and long-lasting luminescence of ~2.7 eV is due to the triplet transition of the F center to the ground state (an analogy with wide-gap oxides) [17–19].

A very large part of the experimental data can be consistently explained on the assumption of the creation and predominant survival under different conditions of synthesis and experiments in real ZnO structures of anionic sublattice defects that determine the state of the surface (sorption of atmospheric gases) and the competition of radiative processes in the UV and visible spectral regions.

Acknowledgement

The work was carried out within the framework of the state task (project 121031500513-4).

5. References

- [1] Ozgur Ü., et al., *J. Appl. Phys.*, **98**, 041301, 2005; doi: 10.1063/1.1992666
- [2] Janotti A., Van de Walle C.G., *Appl. Phys. Lett.*, **87**, 122102, 2005; doi: 10.1063/1.2053360
- [3] Meyer B.K., et al., *Phys. status solidi B*, **241**, 231, 2004; doi: 10.1002/pssb.200301962
- [4] Nikitenko V.A., Kokin S.M., Stoyukhin S.G., Mukhin S.V., *Journal of Applied Spectroscopy*, **87**(5), 796, 2020; doi: 10.1007/s10812-020-01072-5
- [5] Wu X.L., Siu G.G., Fu C.L., Ong H.C., *Applied Physics Letters*, **78**(16), 2285, 2001; doi: 10.1063/1.1361288
- [6] Thomas D.G., *Journal of Physics and Chemistry of Solids*, **15**(1–2), 86, 1960; doi: 10.1016/0022-3697(60)90104-9
- [7] Klingshire C., *Chem. Phys. Chem.*, **8**(6), 782, 2007; doi: 10.1002/cphc.200700002
- [8] Hamby D.W., Lucca D.A., Klopstein M.J., Cantwell G., *Journal of applied physics*, **93**(6), 3214, 2003; doi: 10.1063/1.1545157
- [9] Rodnyi P.A., Khodyuk I.V., *Optics and Spectroscopy*, **111**(5), 776, 2011; doi: 10.1134/S0030400X11120216
- [10] Zhong Y., et al., *The Journal of Physical Chemistry C*, **112**(42), 16286, 2008; doi: 10.1021/jp804132u
- [11] Garces N.Y., et al., *Applied physics letters*, **81**(4), 622, 2002; doi: 10.1063/1.1494125
- [12] Berseth T., Svenson B.G., Kuznetso A.Yu., Klason P., Zhao Q.X., Willander M., *Appl. Phys. Lett.*, **89**, 262112, 2006; doi: 10.1063/1.2424641

- [13] Ton-That C., Weston L., Phillips M.R. *Phys. Rev. B*, **86**, 115205. 2012; doi: 10.1103/PhysRevB.86.115205
- [14] Popov E.A., Kotomin J., *Nuclear Instruments and Methods in Physics Research B*, **268**, 3084, 2010; doi: 10.1016/j.nimb.2010.05.053
- [15] Jin B.J., Bae S., Lee S. Y., Im S., *Materials Science and Engineering: B*, **71**(1–3), 301, 2000; doi: 10.1016/S0921-5107(99)00395-5
- [16] Akopyan I.K., et al., *Physics of the Solid State*, **58**(9), 2016; doi: 10.1134/s1063783416090031
- [17] Noor H., et al., *J. Appl. Phys.* **107**(10), 103717, 2010; doi: 10.1063/1.3428426
- [18] Lushchik A., et al., *Optical Materials: X*, **14**, (2022). 100151, 2022; doi: 10.1016/j.omx.2022.100151
- [19] Seeman V., et al., *Scientific reports*, **10**, 15852, 2020; doi: 10.1038/s41598-020-72958-9